

Amplitude equations of Nikolaevskii turbulence

By

Dan TANAKA*, Hirotoshi AZUMA,** and Hideaki KASAHARA***

Abstract

We numerically integrate amplitude equations for Nikolaevskii-turbulent fluctuations. We show typical spatiotemporal patterns and power spectra. The spatial power spectrum exhibits the same profile as that obtained directly from the Nikolaevskii equation. The temporal power spectrum exhibits non-Lorentzian fluctuations in an intermediate range of frequency. We discuss relation between the Nikolaevskii turbulence and the soft-mode turbulence observed in convective liquidcrystals. Finally, we present a progress report on amplitude equations in higher-dimensional space.

§ 1. In one-dimensional space

The spatiotemporal chaos exhibited by the Nikolaevskii equation [1, 2]

$$(1.1) \quad \partial_t v(x, t) = -\partial_x^2 [\epsilon - (1 + \partial_x^2)^2] v - v \partial_x v$$

results from the interaction between the long-wavelength modes in the stable band on the side of $q = 0$ and the short-wavelength modes in the unstable band surrounding $q = 1$ [3]. This equation includes several issues discussed actively (see the references of [4].) To describe this Nikolaevskii chaos, P. C. Matthews and S. M. Cox derived the amplitude equations

$$(1.2) \quad \partial_t A(x, t) = \epsilon A - i A f + 4 \partial_x^2 A,$$

$$(1.3) \quad \partial_t f(x, t) = -\partial_x (|A|^2) + \partial_x^2 f,$$

2000 Mathematics Subject Classification(s): 2000 Mathematics Subject Classification(s):
Supported by the Ministry of Education, Science, Sports and Culture, Grant-in-Aid for Young
Scientists (Start Up), 18840020, 2006

*Department of Human and Artificial Intelligent Systems (HART), Graduate School of Engineering,
Fukui University 3-9-1 Bunkyo, Fukui 910-8507, Japan.

**2nd Engineering Department, Technical Division, Nichikon Corporation, Kusatsu, Japan.

***System Development Group, Engineering Development Department, AW Engineering Corporation
LTD., Japan.

where A and f represent the slowly varying amplitudes of the two sets of modes:

$$(1.4) \quad v = A(X, T)e^{ix} + \text{c.c.} + f(X, T),$$

where $A = O(\epsilon^{3/4})$, $f = O(\epsilon)$, $\partial_x = O(\epsilon^{1/2})$, and $\partial_t = O(\epsilon)$ [5]. We already confirmed the validity of these scalings [6].

We numerically integrated the rescaled amplitude equations

$$(1.5) \quad \partial_T A(X, T) = A - iAf + \partial_X^2 A,$$

$$(1.6) \quad \partial_T f(X, T) = -\partial_X(|A|^2) + \frac{1}{4}\partial_X^2 f,$$

where we used $A \equiv \epsilon^{3/4}A'$, $f \equiv \epsilon f'$, $X \equiv \epsilon^{1/2}x$, and $T \equiv \epsilon t$ and omitted the prime '. In this equation, the small parameter ϵ does not appear, and for this reason, the integration is computationally less expensive. Although the amplitude equations are ϵ free, we display all the following figures using the original coordinate (x, t) with $\epsilon = 0.01$ for the sake of comparison to results obtained from the Nikolaevskii equation with $\epsilon = 0.01$.

The initial values $A(x, 0)$ and $f(x, 0)$ are small random numbers. In all the figures, the transient time is truncated and the whole space is shown. The boundary condition is periodic.

Figure 1 shows the spatiotemporal pattern of v reproduced from A and f . The corresponding spatial power density spectrum is shown in Fig. 2, where we see that the characteristic chaotic fluctuations of the long-wavelength modes near $q = 0$ and the short-wavelength modes near $q = 1$ are nicely described by the amplitude equations.

Figures 3, 4, and 5 show spatiotemporal patterns of $|A|$, f , and $\text{Re}A$. As we see in Eq. (1.5), f is frequency-like variable for A . This can be seen in the figures: $\text{Re}A$ varies faster when $|f|$ is larger. Also, as we see in Eq. (1.6), f varies faster where the gradient of $|A|$ is larger, which can be seen in the figures. Figure 3 show three white lines which are approximately fixed in space. On these spatial regions, the amplitude is approximately zero for a long period in contrast with the other regions where the amplitude fluctuates rapidly. Also, we see that f is much faster than A as shown in Fig. 3 and Fig. 4.

Figure 6 show the power spectrum $\langle |A_\omega|^2 \rangle$. The soft-mode turbulence in complex electro-hydrodynamic convection exhibits a quite similar onset to that of Nikolaevskii turbulence. Thus, we expect that these two types of turbulence may exhibit the same statistics. However, as shown in Fig. 6, the Nikolaevskii turbulence exhibits non-Lorentzian fluctuations in an intermediate range of frequency in contrast to the soft-mode turbulence exhibiting Lorentzian[7]. Here, we should note that Fig. 6 was obtained from the Matthews-Cox equations Eq. (1.5) and Eq. (1.6) in one-dimensional space. In contrast, the experiments of the soft-mode turbulence are carried out in higher-dimensional space. Thus, we can not simply compare Fig. 6 to the power spectrum of

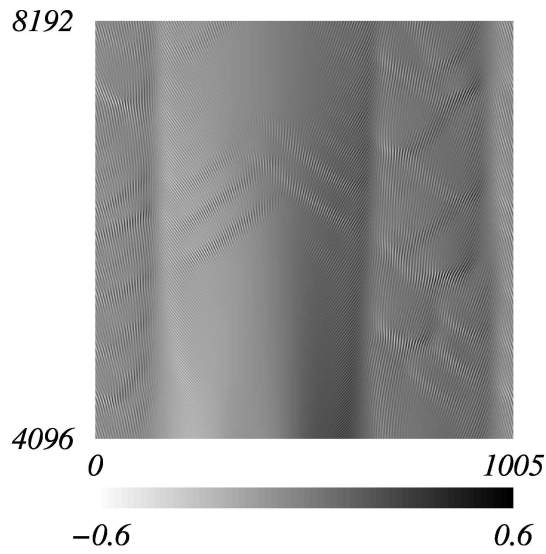


Figure 1. Gray level plots of $v(x, t)$ reproduced from $A(X, T)$ and $f(X, T)$ with $\epsilon = 0.01$. The horizontal and vertical axes correspond to the space $x = \epsilon^{-1/2}X$ and time $t = \epsilon^{-1}T$ respectively.

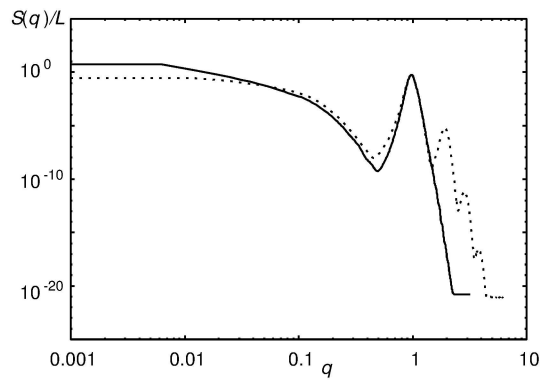


Figure 2. Spatial power density spectra of v obtained from the amplitude equations (bimodal one, solid line) and the Nikolaevskii equation with $\epsilon = 0.01$ (the other one, dotted line), respectively.

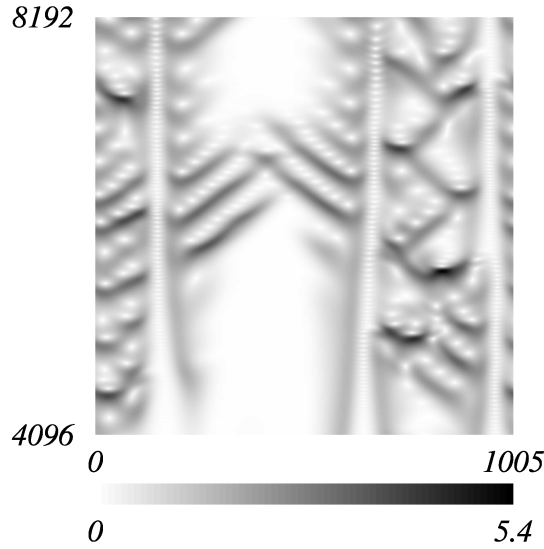


Figure 3. Gray level plots of $A(X, T)$. The horizontal and vertical axes correspond the space $x = \epsilon^{-1/2}X$ and time $t = \epsilon^{-1}T$ with $\epsilon = 0.01$ respectively.

the soft-mode turbulence. To elucidate this subject, we study Nikolaevskii turbulence in higher-dimensional space as follows.

§ 2. In higher-dimensional space

The temporal statistics such as power spectrum proves computationally expensive for the Nikolaevskii equation in higher-dimensional space[8]

$$(2.1) \quad \partial_t \phi(\mathbf{r}, t) = -\nabla_{\mathbf{r}}^2 (\epsilon - (1 + \nabla_{\mathbf{r}}^2)^2) \phi - (\nabla_{\mathbf{r}} \phi)^2,$$

because this equation has the extremely small parameter ϵ which cannot be scale out by using simple translations of variables. Thus, it is appropriate to derive amplitude equations and numerically integrate these equations instead of integrating directly the Nikolaevskii equation in higher-dimensional space. In the following, we present a progress report for the derivation of these amplitude equations.

Fujisaka *et al* derived the amplitude equations[9]:

$$(2.2) \quad \partial_T A(\mathbf{R}, T) = (1 - 4q^2)A + 4 \sum_{\mu, \nu} k_\mu k_\nu \partial_\mu \partial_\nu A + 8iq\mathbf{k} \cdot \nabla A,$$

$$(2.3) \quad \partial_T \phi_0(\mathbf{R}, T) = \nabla^2 \phi_0 + 2|A|^2,$$

$$(2.4) \quad \partial_T \theta(\mathbf{R}, T) = 4\nabla \cdot (q\mathbf{k}) + 2\mathbf{k} \cdot \nabla \phi_0.$$

Here, they assumed $\phi = A(\mathbf{R}, T) \exp[i\theta(\mathbf{r}, T)] + \text{c.c.} + \phi_0(\mathbf{R}, T)$. \mathbf{R}, T are rescaled coordinates in order to describe slow fluctuations. $\nabla_{\mathbf{r}} \theta(\mathbf{r}, T) \equiv \mathbf{k}(\mathbf{R}, T)$ is a local

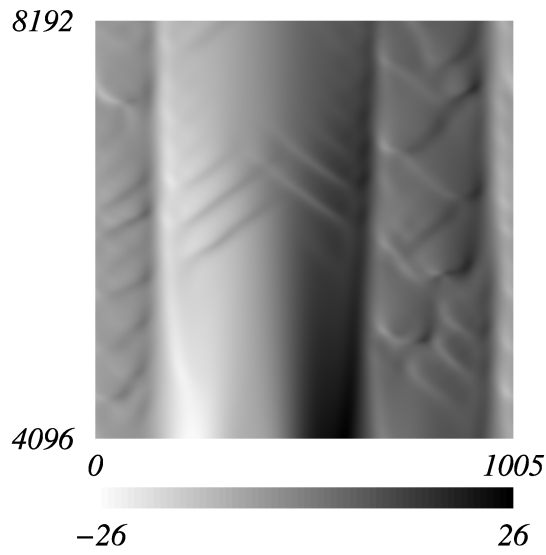


Figure 4. Gray level plots of $f(X, T)$. The horizontal and vertical axes correspond the space $x = \epsilon^{-1/2}X$ and time $t = \epsilon^{-1}T$ with $\epsilon = 0.01$ respectively.

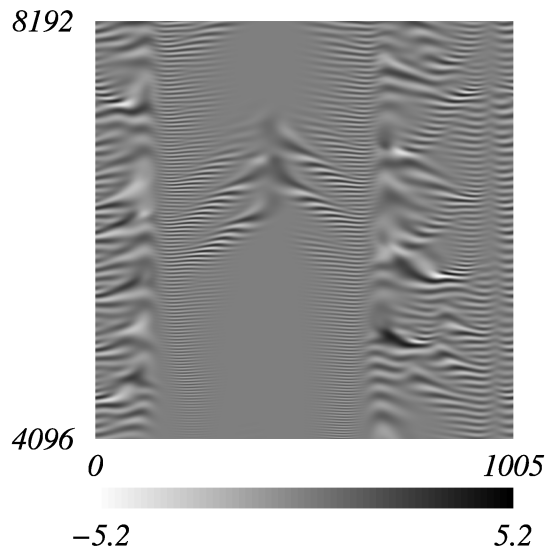


Figure 5. Gray level plots of $\text{Re}A(X, T)$. The horizontal and vertical axes correspond the space $x = \epsilon^{-1/2}X$ and time $t = \epsilon^{-1}T$ with $\epsilon = 0.01$ respectively.

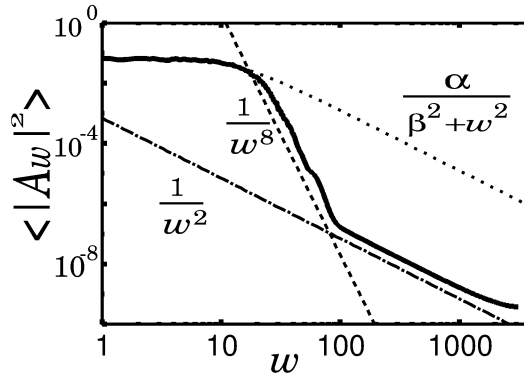


Figure 6. Power spectrum. In an intermediate range of frequency, we found different fluctuations from the Lorentzian. $\alpha = 12.69$, $\beta = 13.61$. The lines $\frac{1}{w^2}$ and $\frac{1}{w^8}$ are shown for the sake of comparison.

wavenumber vector and satisfies $|\mathbf{k}| \sim 1$. q is equal to $\frac{k^2-1}{2\epsilon^{1/2}} \sim 1$. They assumed the following ϵ -scalings: $\mathbf{R} = \epsilon^{1/2}\mathbf{r}$, $T = \epsilon t$, $W \sim \epsilon^{3/4}$, $\phi_0 \sim \epsilon^{1/2}$, $\nabla \cdot \mathbf{k} \sim \epsilon^1$. These five scalings are identical to those in one-dimensional space. They reported that numerical solutions of these amplitude equations diverge. Thus, they added an artificial term $-\sqrt{\epsilon}\nabla \cdot \nabla^2 \mathbf{k}$ to Eq. (2.4) in order to suppress the divergence. This term is extremely small and may not affect the considered modes instead of extremely high wavenumber modes.

Here, we wonder if these assumptions are valid. First, we reconsider the fifth scaling $\nabla \cdot \mathbf{k} \sim \epsilon^1$. This scaling approximately represents

$$(2.5) \quad \frac{|\mathbf{k}(\mathbf{r} + \boldsymbol{\xi}) - \mathbf{k}(\mathbf{r})|}{|\boldsymbol{\xi}|} \sim \frac{\epsilon^{1/2}}{\epsilon^{-1/2}} = \epsilon^1,$$

where ξ is correlation length and is of order $\epsilon^{-1/2}$ because of $\mathbf{R} = \epsilon^{1/2}\mathbf{r}$.

The width of unstable band including the short-wavelength modes ($|\mathbf{k}| \sim 1$) is of order $\sqrt{\epsilon}$. Thus, in one-dimensional space, $|k(x + \xi) - k(x)|$ is reasonably of order $\sqrt{\epsilon}$. However, in higher-dimensional space, the rotation freedom of \mathbf{k} can dominate over its magnitude freedom as shown in Fig. 7. Actually, the soft-mode turbulence in liquid-crystals exhibits patch structures, which correspond to the rotation of \mathbf{k} [10]. If this is the case, $|\mathbf{k}(\mathbf{r} + \boldsymbol{\xi}) - \mathbf{k}(\mathbf{r})|$ must be of order 1. This implies

$$(2.6) \quad \nabla \cdot \mathbf{k} \sim \epsilon^{1/2}.$$

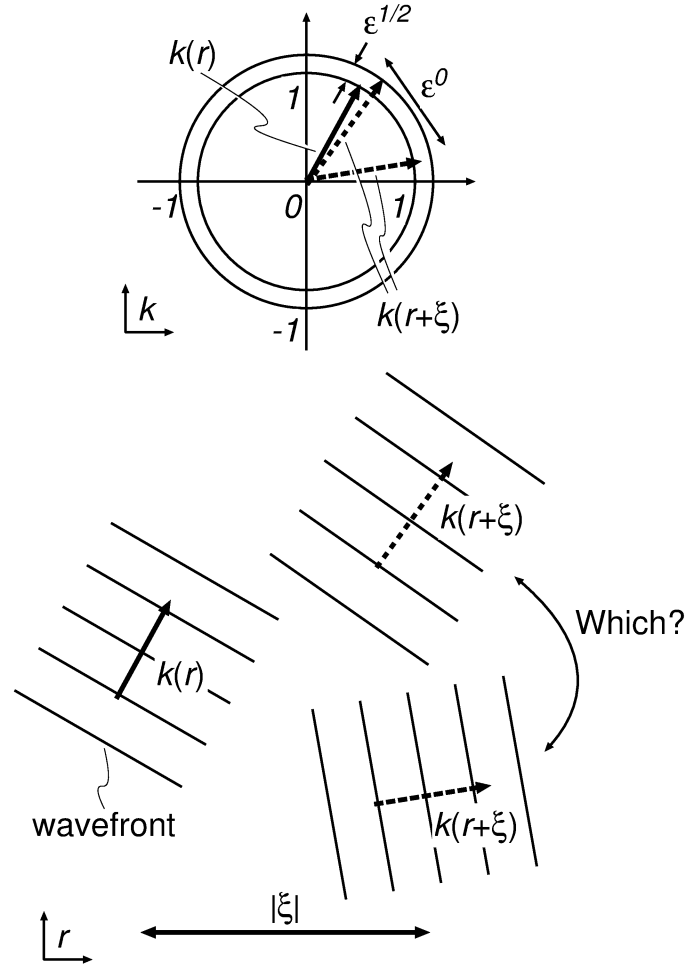


Figure 7. Whether the rotation freedom of \mathbf{k} dominates over its magnitude freedom.

If we adopt this scaling and the other scalings assumed by Fujisaka, we derive

$$(2.7) \quad \partial_T A(\mathbf{R}, T) = (1 - 4q^2)A + 2(\mathbf{k} \cdot \nabla + \nabla \cdot \mathbf{k})^2 + 8iq\mathbf{k} \cdot \nabla A,$$

$$(2.8) \quad \partial_T \phi_0(\mathbf{R}, T) = \nabla^2 \phi_0 + 2|A|^2,$$

$$(2.9) \quad \partial_T \mathbf{k}(\mathbf{R}, T) = 2\nabla[(\mathbf{k} \cdot \nabla)k^2].$$

Here, note that the third equation is closed with \mathbf{k} . When \mathbf{k} is determined by the third equation, the first equation provides the solution of A . This solution of A drives ϕ_0 . We suspect that this type of decoupling is inappropriate for the spatiotemporal chaos.

In order to confirm the validity of Eq. (2.6), we numerically integrate Eq. (2.1) with $\epsilon = 0.01$ in 102.4×102.4 space under periodic boundary conditions. Initial values $\phi(\mathbf{r}, 0)$ are small random numbers. After a transient period, we observe typical spatial patterns as shown in Fig. 8. The spatial structure repeats exhibiting *fishnet*, *flat* (with relatively large value of ϕ), *hexagonal pattern*, and again *fishnet*, \dots . It seems that the

rotation freedom of \mathbf{k} surely dominates over its magnitude freedom.

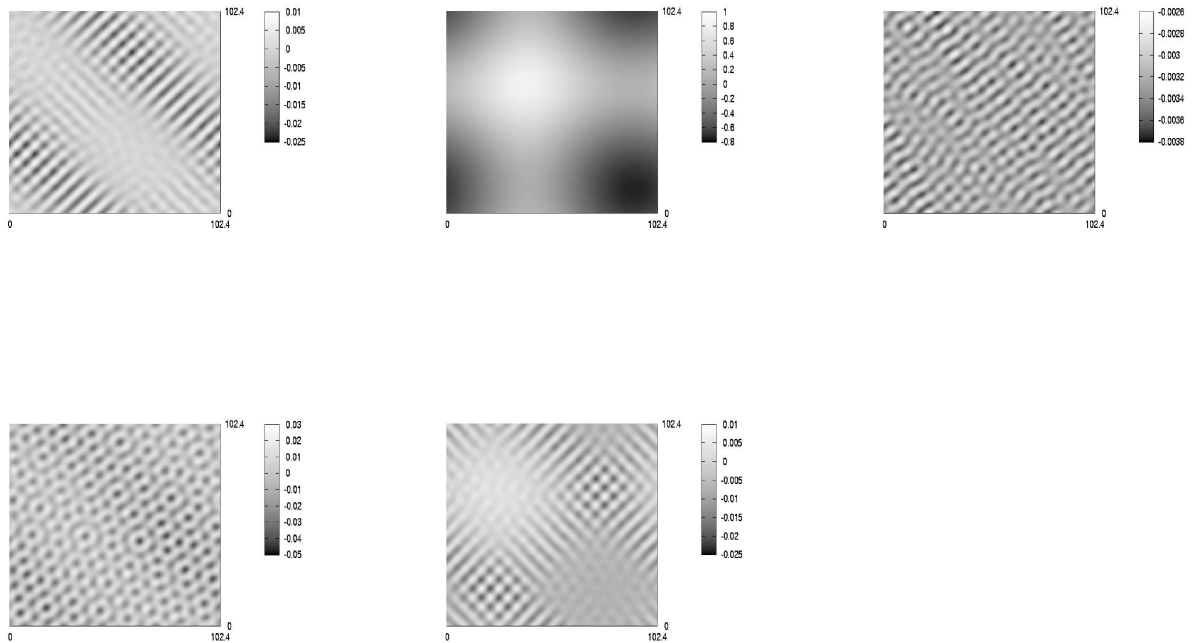


Figure 8. Gray level plots of ϕ obtained from a direct integration of the Nikolaevskii equation with $\epsilon = 0.01$ in two-dimensional space. Top figures, left to right, show snapshots at $t = 56000$, $t = 60000$, and $t = 64000$. Bottom figures, left to right, show snapshots at $t = 68000$, and $t = 72000$.

§ 3. Summary

We numerically integrate Matthews-Cox equations and show that these equations reproduce the spatial power spectrum of the one-dimensional Nikolaevskii turbulence and exhibit the temporal power spectrum that is different from Lorentzian in an intermediate range of frequency. We present a progress report of deriving the amplitude equations for the higher-dimensional Nikolaevskii turbulence. The two types of amplitude equations derived by Fujisaka and us seem to be both inappropriate.

Acknowledgments

D.T. is grateful to H. Fujisaka and M. I. Tribelsky for useful discussions, to S. Kai, Y. Hidaka, and K. Tamura for valuable discussions on their experimental results, to P. Cvitanovic, M. Funakoshi, and S. Cox for encouraging words.

References

- [1] V. N. Nikolaevskii, in *Recent Advances in Engineering Science*, edited by S. L. Koh and C. G. Speciale, Lecture Notes in Engineering Vol.39 (Springer, Berlin, 1989), p. 210.
- [2] D. Tanaka, Phys. Rev. E **70**, 015202 (2004).
- [3] M. I. Tribelsky and M. G. Velarde, Phys. Rev. E **54**, 4973 (1996); M. I. Tribelsky and K. Tsuboi, Phys. Rev. Lett. **76**, 1631 (1996).
- [4] D. Tanaka, Prog. Theor. Phys. Suppl. No.161 119 (2006). D. Tanaka, J. Phys. Soc. Jpn, **74**, 2223 (2005). D. Tanaka, Bussei Kenkyu **84-3**, 437 (2005).
- [5] P. C. Matthews and S. M. Cox, Phys. Rev. E **62**, R1473 (2000).
- [6] D. Tanaka, Phys. Rev. E **71** 025203(R) (2005).
- [7] M. I. Tribel'skii, Phys. Usp. **40**, 159 (1997).
- [8] H. Fujisaka and T. Yamada, Prog. Theor. Phys. **106**, 315 (2001).
- [9] H. Fujisaka, T. Honkawa, and T. Yamada, Prog. Theor. Phys. **109**, 911 (2003).
- [10] K. Tamura *et al.*, J. Phys. Soc. Jpn, **75**, 063801 (2006).